Zooplankton community structure and dominant copepod population structure on the southern Kerguelen Plateau during summer 2016

Kohei Matsuno[a,b,c]*, Jake R. Wallis[c,d], So Kawaguchi[c,e], Sophie Bestley[d,f], Kerrie M. Swadling[c,d]

[a]*Graduate School of Fisheries Sciences, Hokkaido University, 3-1-1 Minato-cho, Hakodate, Hokkaido, 041-8611, Japan*

[b]*Arctic Research Center, Hokkaido University, Kita-21 Nishi-11 Kita-ku, Sapporo, Hokkaido 001-0021, Japan*

[c]*Antarctic Climate & Ecosystems Cooperative Research Centre, 20 Castray Esplanade, Battery Point, Tasmania 7004, Australia*

[d]*Institute for Marine and Antarctic Studies, University of Tasmania, 20 Castray Esplanade, Battery Point, Tasmania 7004, Australia*

[e]*Australian Antarctic Division, 203 Channel Highway, Kingston, Tasmania 7050, Australia*

[f]*CSIRO Oceans and Atmosphere, GPO Box 1538, Hobart Tasmania 7001, Australia*

* Correspondence to: K. Matsuno (k.matsuno@fish.hokudai.ac.jp)

Abstract

The influence of environmental factors on the horizontal community structure of zooplankton over the southern Kerguelen Plateau was investigated during summer in 2016. Zooplankton abundance ranged from 1,490 to 363,484 ind. 1000 m^{-3}, with highest numbers observed in the eastern and central areas. Based on cluster analysis the zooplankton were divided into six groups (A−F), and these were only distinguished based on water masses and frontal systems. Groups A to C had abundant zooplankton and were consistent with areas of high chlorophyll *a* concentration. Group D represented low abundance near the southern Antarctic Circumpolar Current front, while group E was clustered south of the Southern Boundary and group F comprised two stations to the east of the Fawn Trough. Generalised linear model (GLM) highlighted both fronts and chlorophyll *a* concentration as drivers of overall zooplankton distribution. However, the population structures of key species were more likely a result of species-specific life cycles rather than water masses and frontal systems.

Keywords: *Calanoides acutus*, *Calanus propinquus*, *Metridia gerlachei*, *Metridia lucens*, *Rhincalanus gigas*, Fawn Trough, Princess Elizabeth Trough, BANZARE Bank

1. Introduction

The Kerguelen Plateau, and areas to the south, represents one of the most important regions for primary production in the Indian sector of the Southern Ocean (Arrigo et al., 2008), with high stocks of toothfish and krill found in the north and south, respectively (Duhamel et al., 2014; Nicol, 2006). However, the southern Kerguelen Plateau has never been investigated as a single region to determine the distribution and abundances of key species, their habitat characteristics, and the transition between the northern fish-based food web (Pruvost et al., 2005) and the southern krill-based food web (Nicol et al., 2012). Zooplankton play a key role in both food webs, as conduits for transferring energy from primary producers to higher trophic levels. To date, the zooplankton in the southern Kerguelen region have not been well described.

In the Southern Ocean, seawater temperature and variability in sea-ice extent are increasing (Bracegirdle et al., 2008; Turner et al., 2014), although the magnitude and direction of these changes differ among regions around Antarctica (Constable et al., 2014). Zooplankton communities are influenced by the different frontal zones in the Southern Ocean (Errhif et al., 1997; Hunt and Hosie, 2005; Ward et al., 2012; Tachibana et al., 2017), and shifts in the fronts are expected to induce changes in zooplankton distributions (Constable et al., 2014). For example, a modelled 1 °C temperature rise produced a pole-ward shift for all zooplankton taxa (Atkinson et al., 2012). Food web structures are not well understood for the East Antarctic, compared to, for example, the Scotia Sea (Murphy et al., 2007), the Antarctic Peninsula (Ducklow et al., 2006) and the Ross Sea (Smith et al., 2007). Long-term programs such as the Southern Ocean CPR survey (McLeod et al., 2010) have provided information on the patterns of abundance and distribution of zooplankton for much of East Antarctica; however, they do not cover the southern Kerguelen Plateau, the focus of the current study.

The Kerguelen Plateau is an area of significant ecological value, with high krill biomass

to the south (Pauly et al., 2000), and seabirds, seals and whales, using the plateau for migration and feeding (Patterson et al., 2016). The Kerguelen Axis (KAxis) voyage was designed as a synoptic survey, with multiple transects between 57.6 °S and 65.5 °S and 73.3°E and 93.6 °E (Fig 1). The transects encompassed an oceanographically complex region (Park et al., 2009), including the ice-edge, the Southern Boundary (SB) of the ACC and the Southern ACC Front (SAACF). The KAXIS research project aimed to identify and spatially distinguish krill-based and copepod-fish-based food webs and was designed to examine distribution of the food web components from bacteria to mid-trophic levels (fish and squid). This part of the program aimed to describe the horizontal distribution of zooplankton over the Southern Kerguelen Plateau. The population structures of dominant large (> 2 mm) copepods are also presented. Finally, to evaluate the effects of environmental factors on zooplankton distribution, and to determine whether distinct communities were associated with large-scale oceanographic features we applied generalized linear modelling (GLM) and multivariate statistics. This approach has the potential to provide powerful insights into the influence of environmental factors on zooplankton distributions in the Southern Ocean, particularly environmentally variable regions such as the Kerguelen Plateau (Park et al., 2009).

.

2. Materials and Methods

2.1. Field sampling

Thirty-seven sites were sampled over the southern Kerguelen Plateau, including the BANZARE Bank and the Princess Elizabeth Trough, from 23 January to 19 February 2016, onboard the *RSV Aurora Australis* (Fig. 1, Supplementary 1). At each site zooplankton were sampled using an RMT1+8 net, which was deployed by standard double oblique tows from the surface to 200 m. The RMT1 net had a mesh size of 315 μm and mouth area of 1 m^2. The

85 towing speed of the RMT1+8 net ranged between 0.8 and 1.5 m s^{-1} knots (mean = 1.1 m s^{-1}).
86 A flow meter was positioned in the mouth of the RMT8 net to calculate the volume of water
87 filtered; these values were divided by a factor of 9.42 to calculate the volume of water filtered
88 by the RMT1, as per Ikeda et al. (1986). The RMT was fitted with hard cod ends to ensure
89 that the organisms collected were in good condition. Upon retrieval, samples were
90 immediately preserved in 4% buffered formaldehyde solution.
91 A SeaBird SBE911 plus CTD mounted on a SeaBird rosette sampler was deployed at
92 each station to the full depth of the water column (see Bestley et al., 2018 for details).
93 Profiles of salinity, temperature and fluorescence were recorded at each station.
94
95 *2.2 Samples and data analysis*
96 In the laboratory, zooplankton samples were split with a Motoda box splitter so that a
97 minimum of 550 individuals was enumerated per sample. Zooplankton were identified to
98 species level where possible and counted under a stereomicroscope (Leica M165C). Large-
99 sized copepods (adults >2 mm; i.e. *Calanoides acutus*, *Calanus propinquus*, *Calanus*
100 *simillimus*, *Metridia gerlachei*, *Metrida lucens* and *Rhincalanus gigas*) were identified to
101 copepodite stage. To identify the zooplankton, we referred to Razouls (1994) for copepods,
102 Kirkwood (1982) for euphausiids and Boltovskoy (1999) for other species. Abundance is
103 reported as the number of individuals 1000 m^{-3}.
104 The mean copepodid stage (*MCS*) of the six large copepods was calculated for each station
105 where they occurred using the following equation:

106 $$MCS = \frac{\sum_{i=1}^{6} i \times Ai}{\sum_{i=1}^{6} Ai} \quad (1)$$

107 where *i* is the copepodite stage (1-6 indicates copepodid stage 1− copepodid stage 6), and *Ai*
108 is the abundance (ind. 1000 m^{-3}) of the *i*th copepodid stage (Marin, 1987).

Multivariate analyses, designed to explore relationships between zooplankton and their environment, were performed with PRIMER v7 (PRIMER-e). Abundance of each taxon was fourth-root transformed prior to cluster analysis to reduce the effect of abundant species (Quinn and Keough, 2002). A similarity matrix based on stations was constructed using the Bray-Curtis index, which is useful for biological data when there are many zeros (Quinn and Keough, 2002). For grouping the samples (Q-mode analysis), the similarity indices were coupled with hierarchical agglomerative clustering using a complete linkage method: Unweighted Pair Group Method using Arithmetic mean (UPGMA; Field et al., 1982). Accompanying this analysis, similarity profile analysis (SIMPROF) was added to determine if groupings of the stations were statistically significant (at 5% significance level). Similarity percentages (SIMPER) analysis was applied to determine which species contributed to the top 50% of total abundance for each group. Non-metric multi-dimensional scaling (NMDS) with multiple regression analysis was undertaken to explore relationships between the sampling sites and environmental data.

Regional differences in mean abundance among groups were tested by one-way ANOVA and the Tukey-Kramer post-hoc test was applied to distinguish which groups were statistically different. Additionally, a Mann-Whitney U-test was performed on abundance between the clustering groups (A-C vs D-F) using R (version 3.4.0; R Core Team, 2017).

To find potential indicator species in the groups that resulted from the cluster analysis, the program Indicator Value (IndVal) was applied (Dufrêne and Legendre, 1997). IndVal was calculated as:

$$IndVal_{ij}=A_{ij}*B_{ij}*100 \quad (2)$$

Where $A_{ij}=Nindividuals_{ij}/Nindividuals_i$, and $B_{ij}=Nsite_{ij}/Nsites_j$.

A_{ij} is a measure of site specificity, where $Nindividuals_{ij}$ is the mean number of individuals in species *i* across sites of group *j*, and $Nindividuals_i$ is the sum of the mean numbers of

134 individuals of species *i* over all groups. B_{ij} is a measure of group fidelity, where $Nsite_{ij}$ is the
135 number of sites in group *j* where species *i* is present, while $Nsite_j$ is the total number of sites
136 in that group (Dufrêne and Legendre, 1997).
137 To evaluate the effects of environmental drivers on zooplankton community
138 structure, we applied generalised linear models (GLMs, R version 3.4.0; R Core Team, 2017).
139 To run the GLMs for each taxon we used a negative binominal distribution based on count
140 data, with filtered volume applied as an offset. *MCS* of the copepods were tested based on the
141 Gaussian distribution. We tested for overdispersion by calculating the dispersion parameter
142 (Pearson's chi-square statistic / degrees of freedom in residual deviance) and found that
143 values were close to 1 (0.89 - 1.34), indicating the models captured most of the variation.
144 Only radiolarians had a dispersion parameter (1.89) that justified their removal from further
145 GLM. The following factors were included in the GLM: depth (of the water column);
146 chlorophyll *a* concentration (chl.*a*) as a measure of food availability; density averaged over
147 the top 10 dbar, where low values can indicate recent sea ice melt; $salinity_{200}$, which has a
148 direct effect on zooplankton physiology; MLD (mixed layer depth) as shallower depths can
149 enhance primary production leading to more food for zooplankton; $Temp_{200}$, average
150 temperature over the top 200 m as zooplankton metabolism is coupled tightly to temperature;
151 time since melt, with the ice edge a region of high productivity and enhanced food supply;
152 SST (sea surface temperature); and PAR (photosynthetically active radiation), as time when
153 zooplankton are sampled can influence their position in the water column. Further details for
154 defining each of these environmental variables are shown in Table 1. To remove
155 multicollinearity among the environmental parameters we calculated variance inflation
156 factors (VIF) for each parameter. If the VIF was higher than 3, it was removed from the
157 explanatory parameters (O'Brien, 2007). To derive the final model, full models with all
158 environmental variables were first constructed. Then, model selection was applied by

159 "stepAIC" in the "MASS" package to choose the final models. Comparison between null and
160 final models by ANOVA confirmed the goodness of fit of the model. If the p value <0.05,
161 then the final model was deemed to be better than the null model.

162 **3. Results**

163 *3.1. Spatial changes in hydrographic condition*

164 The surface mixed layer (SML) varied among stations, with the deepest at KX34 (68 m) and
165 the shallowest at KX18-20 (13 m; Fig 2a). Across the sampling region, the mean temperature
166 of the upper 20 m of the water column (defined as SST) ranged from -1.68 to 3.75 °C; the
167 north-east area was warmest, while the southern area was cooler (Fig. 2b). The mean
168 temperature averaged over the top 200 m of the water column (Fig. 2c) had a smaller range (-
169 1.65 to 1.76 °C) compared with the top 20 m, while Mean salinity in the top 200 m ranged
170 from 34 to 34.48, with the north-east area being slightly fresher (Fig. 2d). Mean density in the
171 upper SML ranged from 26.309 to 27.144 kg m^{-3}, indicting recent ice melt (Fig. 2e). Finally,
172 Integrated chlorophyll *a* ranged from 19.7 to 132.8 mg m^{-2}, with stations KX04-KX09, KX39
173 and KX47 having concentrations higher than 100 mg m^{-2} (Fig. 2f).

174 *3.2 Spatial changes in the zooplankton community*

175 Total zooplankton abundance ranged from 1,490 to 363,484 ind. 1000 m^{-3}, with the lowest
176 abundance at KX43, and the largest at KX15 (Fig. 3a). Higher abundances were observed in
177 the eastern and central areas. The zooplankton community was divided into 6 groups (A−F)
178 at 75.7 and 78.7% similarity by Q-mode cluster analysis with SIMPROF, based on
179 zooplankton abundances at each site (Fig. 4a). Based on one-way ANOVA and a Tukey-
180 Kramer post-hoc test, the abundances of groups A and C were significantly higher than those
181 of the remaining four groups (B, D-F; p<0.0001). Additionally, the mean abundance of

groups A-C was about 10 times higher than that of groups D-F (67,230±79,473 vs 6,193± 4035 ind. 1000 m^{-3}; Mann-Whitney U-test, $p<0.01$). Copepods were the dominant taxon in all six groups (59-76%), while foraminifera were the next most abundant group (4-31%; Fig. 4b). NMDS showed clear separation among the groups, with low stress (0.11). Five environmental factors, namely latitude, longitude, temperature, salinity and fluorescence, had correlations of $R^2 > 0.3$ with the groups based on associations among stations. The distribution of the groups across the sampling region broadly corresponded to water mass distribution (Fig. 5). Groups A, B and C were observed in the central and eastern areas, north of the subpolar zone and along the Kerguelen Plateau. Group D occurred in the central region, mainly in the northern part of the transect. Group E was observed from the Antarctic Slope Current to the Southern Boundary front, while Group F was located in the Fawn Trough Current.

Based on the SIMPER analysis the copepods *Calanoides acutus*, *Calanus propinquus*, *Calanus simillimus*, *Ctenocalanus* spp., *Metridia gerlachei*, *Metridia lucens*, *Oithona* spp., *Oncaea* spp. and *Rhincalanus gigas,* the chaetognath *Eukrohnia hamata*, the euphausiid *Thysanoessa macrura*, radiolarians and foraminiferans were all important contributors to at least one group (Table 2). Foraminifera was the dominant taxon in four groups (A-D), while *C. acutus* was the second dominant species in groups A-C. *Oithona* spp. was the second dominant taxon in group D, and *M. gerlachei* was dominant in group E; *Ctenocalanus* spp. and *C. simillimus* were the dominant species in group F.

3.3. Spatial distribution of large-sized copepods

Calanoides acutus occurred at all stations along the transect, predominantly around the central region, with *MCS* values falling between CIII and CIV in the northwest and around CV towards the southeast (Fig. 6). *Calanus propinquus* also occurred at all stations, with

206 younger copepodid stages more prelavent than for the *C. acutus* population (3.05±0.54 vs
207 3.54±0.72, Mann-Whitney U-test, $p<0.01$). *Calanus simillimus* was observed at only nine
208 stations, most of them north of the Southern Boundary and mainly to the east of plateau; *MCS*
209 was > 4. *Metridia gerlachei* occurred at all stations and was abundant on the eastern-most
210 transect and close to the continent; its average *MCS* was ~ 4. *Metridia lucens* had a more
211 northerly distribution than *M. gerlachei*, and its *MCS* ranged between 3.2 and 5. *Rhincalanus*
212 *gigas* occurred at all stations, though in lower numbers than *C. acutus* and *C. propinquus*
213 (728±832 vs 6,262±12,834 and 2,989±4,737 ind. 1000 m^{-3}, respectively). The mean *MCS*
214 of *R. gigas* (4.5±0.67) was higher than those of *C. acutus* and *C. propinquus*.

215 *3.4 Environmental drivers of the zooplankton community*

216 Summaries of the results from the GLM are shown in Tables 3 and 4. For total zooplankton at
217 each site higher abundances were generally associated with warmer temperatures, higher
218 chlorophyll *a*, shallower depths and decreased light intensity (night). When split into the
219 main taxonomic groups, the effects of environmental drivers were similar to those shown for
220 total zooplankton abundance. For euphausiacea, higher abundance was observed at stations
221 where the mixed layer depths were shallow. The GLMs showed that abundances of five of the
222 large-size (> 2 mm) copepods (modelled separately), responded in a similar fashion to the
223 total copepod group, although *M. gerlachei* showed higher abundances with cooler
224 temperatures in the top 200 m of the water column. *Calanoides acutus* and *M. lucens* had
225 increased abundance at stations where sea ice had persisted for longer.

226 For the mean copepodid stages of the large-sized copepods, the effects of
227 environmental drivers varied with species. *Calanoides acutus* showed two positive (density
228 and time since melt) and three negative relations ($Temp_{200}$, MLD, and chl.*a*), while *C.*
229 *propinquus* exhibited one positive (Density) and two negative relationships ($Salinity_{200}$ and

SST). *Metridia gerlachei* had a weak positive relationship with $Temp_{200}$ and *M. lucens* had one positive (SST) and one negative (Depth). Younger stages in *R. gigas* occurred at stations were the MLD was shallower.

4. Discussion

4.1. Effects of water masses and frontal systems on zooplankton community

Studies of zooplankton on the southern Kerguelen Plateau are limited. Swadling et al. (2010) investigated the zooplankton community based on RMT1 samples to the region west (BROKE-West; 30–80°E) of the current study (71.2-93.6°E) during summer in 2006. In that survey, foraminifera, small copepods and appendicularians dominated the zooplankton community, while euphausiids (*Euphausia crystallorophias*) and the copepod *Metridia gerlachei* were highlighted as indicator species (Swadling et al., 2010). In the present study appendicularians were three orders of magnitude lower than observed in the BROKE-West study, while foraminiferans and radiolarians were much more abundant. Appendicularians have a short generation time (e.g., eight days at 15 °C), which increases in colder temperatures (Deibel and Lowen, 2012). In polar regions, they can develop quickly and time their reproduction to the ice-edge phytoplankton bloom (Acuña et al., 1999); after reproduction their abundance decreases rapidly following end of the phytoplankton bloom. One hypothesis is that the lower numbers of appendicularians observed in the present study reflect some of the sites being sampled after the end of the phytoplankton bloom.

High numbers of foraminifera are found in the sea ice of the Southern Ocean, and they release into the water column with sea-ice melt (Ojima et al., 2017). This fact suggests foraminifera might be abundant where sea ice cover persisted for the longest time and cells were released during the ice melt. Given that days after melt were generally lower than those recorded in Swadling et al. (2010) it might explain why the abundances recorded in the

254 present study were up to 20 times higher than reported for BROKE-West. In spite of this we
255 did not see a significant relationship between the ice-melt indices (i.e., Density and Time
256 since melt) and abundance of foraminiferans. This might be explained by the fact that
257 foraminifera are known to be influenced by many environmental factors, including snow
258 depth and chl. *a* in the water column (Wallis et al., 2016). In our study, foraminifera were
259 abundant in areas with high primary production, indicating that feeding preferences of
260 foraminiferans might be an important driver.

261 The zooplankton communities found across the Southern Kerguelen Plateau in
262 summer 2016 were split into two groups via multivariate analyses (groups A−C vs groups
263 D−F) based on abundance. The distribution of the high-abundance group (i.e., groups A−C)
264 was consistent with the distribution of high chl. *a*, highlighting possible foodweb interactions
265 where the zooplankton were tracking the higher concentrations of phytoplankton. The GLM
266 showed that total abundance of zooplankton was positively influenced by water-mass indices
267 (i.e., $Temp_{200}$), lower light intensity (i.e., PAR) and increased phytoplankton biomasss (i.e.,
268 chl.*a*). The negative effect of light intensity on abundance suggested most species performed
269 diel vertical migration during summer, whereby they were distributed deeper in the water
270 column during the day (Takahashi et al., 2017). According to Swadling et al. (2010), the
271 zooplankton community between 30 °E and 80 °E was correlated with chlorophyll *a*
272 concentration, proximity to the Antarctic Slope Current and length of time without an ice
273 cover. Thus, the zooplankton community across the western side of the Indian sector appears
274 to be governed by the interplay of frontal systems, their vertical migration and bottom-up
275 factors affecting productivity around the Kerguelen Plateau during summer.

276 Zooplankton assemblages are closely related to the different frontal zones in the
277 Southern Ocean (Hunt and Hosie, 2005, 2006a, b; Hosie et al., 2014; Tachibana et al., 2017).
278 Around the Kerguelen Plateau, several currents and frontal zones are observed (Park et al.,

2009; Bestley et al., 2018). The Antarctic Circumpolar Current (ACC) is disrupted by the plateau, which forces the core of the ACC to pass along its northern escarpment (e.g., Park et al., 1993). Following that, the southern Antarctic Circumpolar Current front (sAACf) and the Southern Boundary (SB) extend northward on the eastern edge of the Kerguelen Plateau. The Fawn Trough Current flows southeasterly at the north-east of the Kerguelen Plateau (Roquet et al., 2009). However, zonal homogeneity is broken by features such as gyres (Kaiser et al., 2009). These features of complicated oceanographic conditions potentially relate to zooplankton distribution. In this study the Southern Boundary clearly divided the zooplankton assemblages in the south-east region, while the central region was more homogeneous. This implies that a stable frontal system was present in the south-east region, while an unstable system induced gyres in the central region (Bestley et al., 2018).

4.2. Environmental drivers of zooplankton abundance and population structure of large-sized copepods

Population structure reflects growth and reproductive capacity and assists in our understanding of life cycles and the condition of a population (e.g., Atkinson, 1989). Mean copepodid stage (*MCS*) of copepods is a useful index for evaluating their population structure, with the value decreasing with input of new generations by reproduction and increasing with ontogenetic development within the population.

Calanoides acutus and *C. propinquus* are distributed widely in the Southern Ocean, from the Polar Front to the Antarctic coast; however, they are usually more abundant north of the SB-ACC and decrease towards the continent (e.g., Atkinson, 1996; Hosie et al., 2000; Tanimura et al., 2008). In the present study, these two species were mainly found north of the Southern Boundary, and their population structures were similar in terms of abundance and *MCS*. Wallis et al. (2016) reported a positive influence on *C. propinquus* abundance from

303 chl.*a* in water and sea ice, snow depth, latitude and year. In the present study, *C. propinquus*
304 showed positive relationships with average temperature in the top 200 m and chlorophyll
305 concentration, and negative relationships with average salinity, surface temperatures, water
306 column depth and PAR. This species migrates into the surface layer in spring and reproduces,
307 before descending into the deep layer for diapause during autumn (Schnack-Schiel et al.,
308 1991, Atkinson, 1996). While the environmental drivers of abundances of *C. acutus* and *C.*
309 *propinquus* were similar, the sea-ice melt indices (Density and Time since melt) showed
310 negative relationships only with *C. acutus* abundances and positive relationships with their
311 *MCS*. Thus, higher abundance of the younger stages was associated with lower surface
312 density, suggesting a shorter time since sea-ice melt. *Calanoides acutus* reproduces from
313 November to March in the Weddell Sea (Hagen and Schnack-Schiel, 1996), and the
314 appearance of the cohort likely coincides with the high chlorophyll *a* concentration in the
315 summer period (Atkinson, 1998). *Calanus simillimus* occurred in the north-east regions,
316 particularly near the Fawn Trough Current. This species might have been transported south
317 from more northerly warmer waters, because it is known to be distributed in subantarctic
318 waters and northern parts of the ACC (Atkinson, 1998).

319 The two species of *Metridia* had different distributions: *M. gerlachei* was dominant
320 in the south, while *M. lucens* had higher abundances in the north, a common pattern in the
321 Southern Ocean (e.g., Atkinson, 1989). The GLM results indicated that abundance of *M.*
322 *gerlachei* showed similar responses to those of *C. propinquus*, except for the effects of
323 temperature: higher temperatures in the lower mixed layer resulted in higher abundance of *C.*
324 *propinquus* and lower abundance of *M. gerlachei*. Light intensity did not have a strong
325 influence on *Metridia* species compared to the other copepods. This was interesting because
326 this genus is known to undertake diel vertical migration rather than seasonal vertical
327 migration (Atkinson and Peck, 1988; Huntley and Escritor, 1992; Schnack-Schiel and Hagen,

328 1995). The *MCS* for the two *Metridia* species were high and might not relate directly to
329 chlorophyll distribution because these species have a long reproductive period (i.e., there is
330 no clear reproductive-peak season) and distribute rather patchily without any apparent link to
331 the distribution of chlorophyll (Atkinson, 1989, 1998). For *Rhincalanus gigas*, late copepodid
332 stages were dominant, although their nauplii were observed in almost all samples (data not
333 shown). The reproduction of this species is reported to occur mainly during summer
334 (Atkinson, 1998), though with regional differences; e.g. reproduction continues into late
335 autumn around the Antarctic Peninsula (Martin and Schnack-Schiel, 1993). *Rhincalanus*
336 *gigas* was reproducing during the January and February in the Indian sector. From the GLM,
337 the relationships of *R. gigas* with environmental drivers was similar to the other copepods,
338 although chlorophyll *a* concentration was not a strong influence on this species.
339 Recently, research investigating environmental drivers of zooplankton abundance in
340 the Southern Ocean via statistical modelling (e.g., GLM, generalised additive models) has
341 increased (e.g., Wallis et al. 2016; Kelly et al. this issue), but studies using aspects of
342 population structure (e.g., MCS) as a response variable in GLM are limited. In this study, the
343 discussion of population structure was augmented by comparing the environmental drivers of
344 developmental stages of copepods using GLM. Thus, GLM is a powerful analytical tool
345 capable of distinguishing structure within copepod populations even within complex
346 oceanographic regions such as the south Kerguelen Plateau. Also, GLM helped determine
347 those conditions that are most suited to each taxonomic assemblage. This information is
348 useful for identifying productive regions and understanding the response of zooplankton to
349 environmental change. In future, detailed information (e.g., population structure) for the main
350 zooplankton species should be monitored and used in assessing the influence of climate
351 change on key zooplankton species.

Acknowledgements

We thank the Science Technical Support Team of the Australian Antarctic Division and the master and crew of the RV *Aurora Australis* for their considerable efforts to support this research. This study was supported by AAS Grants 4331 and 4344. This project was also supported by the Australian Government's Business Cooperative Research Centres Programme through the Antarctic Climate and Ecosystems Cooperative Research Centre, and the Australia Research Council's Special Research Initiative for Antarctic Gateway Partnership (Project ID SR140300001). Part of the present study was financially supported through Overseas Research Fellowships and a Grant-in-Aid for Scientific Research 18K14506 (Early Career Scientists) from the Japanese Society for Promotion of Science (JSPS). This project was also supported by the Australian Governments Cooperative Research Centres Program, through the Antarctic Climate and Ecosystems CRC. Three anonymous reviewers substantially improved this manuscript.

References

Acuña, J.L., Deibel, D., Bochdansky, A.B., Hatfield, E., 1999. *In situ* ingestion rates of appendicularian tunicates in the northeast water Polynya (NE Greenland). Mar. Ecol. Prog. Ser. 186, 149−160.

Arrigo, K.R., Van Dijken, G.L., Bushinsky, S., 2008. Primary production in the Southern Ocean, 1997–2006. J. Geophys. Res. 113, C08004.

Atkinson, A., 1989. Distribution of six major copepod species around South Georgia in early summer. Polar Biol. 9, 353−363.

Atkinson, A., 1996. Subantarctic copepods in an oceanic, low chlorophyll environment: ciliate predation, food selectivity and impact on prey populations. Mar. Ecol. Prog. Ser. 130, 85−96.

Atkinson, A., 1998. Life cycle strategies of epipelagic copepods in the Southern Ocean. J. Mar. Syst. 15, 289−311.

Atkinson, A., Peck, J.M., 1988. A summer-winter comparison of zooplankton in the oceanic area around South Georgia. Polar Biol. 8, 463−473.

Atkinson, A., Ward, P., Hunt, B.P.V., Pakhomov, E.A., Hosie, G.W. 2012. An overview of Southern Ocean zooplankton data: abundance, biomass, feeding and functional relationships. CCAMLR Science 19, 171−218.

Bestley, S., van Wijk, E., Rosenberg, M., Eriksen, R., Corney, S., Tattersall, K., Rintoul, S., 2018. Ocean circulation and frontal structure near the southern Kerguelen Plateau: The physical context for the Kerguelen Axis ecosystem study. Deep-Sea Res. II, https://doi.org/10.1016/j.dsr1012.2018.1007.1013.

Boltovskoy, D., (Ed.) 1999. South Atlantic Zooplankton volumes 1 & 2, Backhuys, Leiden.

Bracegirdle, T.J., Connolley, W.M., Turner, J., 2008. Antarctic climate change over the twenty-first century. J. Geophys. Res. 113, D03103.

390 Cavalieri, D.J., Parkinson, C.L., Gloersen, P., Zwally, H.J., 1996. updated yearly. Sea Ice
391 Concentrations from Nimbus-7 SMMR and DMSP SSM/I-SSMIS Passive Microwave
392 Data, Version 1. [January - February 1997 - 2015]. NASA National Snow and Ice Data
393 Center Distributed Active Archive Center. Boulder, Colorado USA.
394 Constable, A.J., Melbourne-Thomas, J., Corney, S.P., Arrigo, K.R., Barbraud, C., Barnes, D.
395 K., Bindoff, N.L., et al. 2014. Climate change and Southern Ocean ecosystems I: how
396 changes in physical habitats directly affect marine biota. Glob. Change Biol. 20,
397 3004−3025.
398 de Boyer Montégut, C., Madec, G., Fischer, A.S., Lazar, A., Iudicone, D., 2004. Mixed layer
399 depth over the global ocean: An examination of profile data and a profile-based
400 climatology. J. Geophys. Res. 109, C12003.
401 Deibel, D., Lowen, B., 2012. A review of the life cycles and life-history adaptations of
402 pelagic tunicates to environmental conditions. ICES J. Mar. Sci. 69, 358−369.
403 Ducklow, H.W., Fraser, W., Karl, D.M., Quetin, L.B., Ross, R.M., Smith, R.C., Stammerjohn,
404 S.E., Vernet, M., Daniels, R.M., 2006. Water-column processes in the West Antarctic
405 Peninsula and the Ross Sea: interannual variations and foodweb structure. Deep-Sea
406 Res. Part II, 53, 834-852.
407 Dufrêne, M., Legendre, P., 1997. Species assemblages and indicator species: the need for a
408 flexible asymmetrical approach. Ecol. Monogr. 67, 345−366.
409 Duhamel, G., Hulley, P.-A., Causse, R., Koubbi, P., Vacchi, M., Pruvost, P., Vigetta, S.,
410 Irisson. J.-O., Mormède, S., Belchier, M., Dettai, A., Detrich, H.W., Gutt, J., Jones,
411 C.D., Kock, K.-H., Lopez, Abellan, L.J., Van de Putte, A.P., 2014. Chapter 7.
412 Biogeographic Patterns of Fish, in: De Broyer, C., Koubbi, P., Griffiths, H.J., Raymond,
413 B., Udekem d'Acoz C. d', Van de Putte, A.P., Danis, B., David, B., Grant, S., Gutt, J.,
414 Held, C., Hosie, G., Huettmann, F., Post, A., Ropert-Coudert, Y. (Eds.), Biogeographic

Atlas of the Southern Ocean. Scientific Committee on Antarctic Research, Cambridge, pp. 328−362.

Errhif, A., Razouls, C., Mayzaud, P., 1997. Composition and community structure of pelagic copepods in the Indian sector of the Antarctic Ocean during the end of the austral summer. Polar Biol. 17, 418−430.

Field, J.G., Clarke, K.R., Warwick, R.M., 1982. A practical strategy for analyzing multispecies distribution patterns. Mar. Ecol. Prog. Ser. 8, 37−52.

Hagen, W., Schnack-Schiel, S.B., 1996. Seasonal lipid dynamics in dominant Antarctic copepods: Energy for overwintering or reproduction? Deep-Sea Res. I 43, 139−158.

Hosie, G.W., Schultz, M.B., Kitchener, J.A., Cochran, T.G., Richards, K., 2000. Macrozooplankton community structure off East Antarctica (80−150°E) during the Austral summer of 1995/1996. Deep-Sea Res. II 47, 2437−2463.

Hosie, G., Mormède, S., Kitchener, J., Takahashi, K., Raymond, B., 2014. 10.3. Near-surface zooplankton communities, in: De Broyer, C., Koubbi, P., Griffiths, H.J., Raymond, B., Udekem d'Acoz C. d', Van de Putte, A.P., Danis, B., David, B., Grant, S., Gutt, J., Held, C., Hosie, G., Huettmann, F., Post, A., Ropert-Coudert, Y. (Eds.), Biogeographic Atlas of the Southern Ocean. Scientific Committee on Antarctic Research, Cambridge, pp 422−430.

Hunt, B., Hosie, G. 2005. Zonal structure of zooplankton communities in the Southern Ocean South of Australia: results from a 2150 km continuous plankton recorder transect. Deep-Sea Res. I 52, 1241−1271.

Hunt, B., Hosie, G., 2006a. The seasonal succession of zooplankton in the Southern Ocean south of Australia, part I: the seasonal ice zone. Deep Sea Res. I, 53, 1182−1202.

Hunt, B., Hosie, G., 2006b. The seasonal succession of zooplankton in the Southern Ocean south of Australia, part II: the sub-antarctic to Polar Frontal Zones. Deep Sea Res. I 53,

1203−1223.

Huntley, M.E., Escritor, F., 1992. Ecology of *Metridia gerlachei* Giesbrecht in the western Bransfield Strait, Antarctica. Deep-Sea Res. 39, 1027−1055.

Ikeda, T., Hosie, G., Stolp, M., 1986. SIBEXII cruise krill/zooplankton data. ANARE Research Notes 32, 1–70.

Kaiser, S., Barnes, D.K.A., Sands, C.J., Brandt, A., 2009. Biodiversity of an unknown Antarctic Sea: assessing isopod richness and abundance in the first benthic survey of the Amundsen continental shelf. Mar. Biodiv. 39, 27. https://doi.org/10.1007/s12526-009-0004-9.

Kelly, P., Corney, S.P., Melbourne-Thomas, J., Kawaguchi, S., Bestley, S., Fraser, A., Swadling, K.M., this issue, Salpa thompsoni in the Indian Sector of the Southern Ocean: environmental drivers and life history parameters. Deep-Sea Res. II.

Kirkwood, J.M., 1982. A guide to the Euphausiacea of the Southern Ocean (No. 1-5). Information Services Section, Antarctic Division, Dept. of Science and Technology.

Marin, V., 1987. The oceanographic structure of eastern Scotia Sea-IV. Distribution of copepod species in relation to hydrography in 1981. Deep-Sea Res. 34, 105–121.

Martin, V.H., Schnack-Schiel, S.B., 1993. The occurrence of *Rhincalanus gigas*, *Calanoides acutus*, and *Calanus propinquus* (Copepoda: Calanoida) in late May in the area of the Antarctic Peninsula. Polar Biol. 13, 35−40.

Maslanik, J., Stroeve, J., 1999. updated daily. Near-Real-Time DMSP SSMIS Daily Polar Gridded Sea Ice Concentrations, Version 1. [January - February 2016]. Boulder, Colorado USA. NASA National Snow and Ice Data Center Distributed Active Archive Center. Boulder, Colorado USA.

McLeod, D.J., Hosie, G.W., Kitchener, J.A., Takahashi, K.T., Hunt, B.P.V. 2010. Zooplankton atlas of the Southern Ocean: the SCAR SO-CPR survey (1991–2008). Polar Sci. 4, 353-

385.

Murphy, E.J., Watkins, J.L., Trathan, P.N., Reid, K., Meredith, M.P., Thorpe, S.E., Johnston, N.M., Clarke, A., Tarling, G.A., Collins, M.A., Forcada, J., Shreeve, R.S., Atkinson, A., Korb, R., Whitehouse, M.J., Ward, P., Rodhouse, P.G., Enderlein, P., Hirst, A.G., Martin, A.R., Hill, S.L., Staniland, I.J., Pond, D.W., Briggs, D.R., Cunningham, N.J., and Fleming, A.H., 2007. Spatial and temporal operation of the Scotia Sea ecosystem: a review of large-scale links in a krill centred food web. Phil. Trans. Royal Soc. London Series B, 362, 113-148.

Nicol, S., 2006. Krill, currents, and sea ice: *Euphausia superba* and its changing environment. BioScience 56, 111−120.

Nicol, S., Foster, J., Kawaguchi, S., 2012. The fishery for Antarctic krill – recent developments. Fish Fish. 13, 30−40.

O'Brien, R.M., 2007. A caution regarding rules of thumb for variance inflation factors. Qual. Quant. 41, 673−690.

Ojima, M., Takahashi, K.T., Iida, T., Moteki, M., Miyazaki, N., Tanimura, A., Odate, T., 2017. Variability of the fauna within drifting sea ice floes in the seasonal ice zone of the Southern Ocean during the austral summer. Polar Sci. 12, 19−24.

Park, Y.-H., Gambéroni, L., Charriaud, E., 1993. Frontal structure, water masses and circulation in the Crozet Basin. J. Geophys. Res. 98, 12361−12385, doi:10.1029/93JC00938.

Park, Y.-H., Vivier, F., Roquet, F., Kestenare, E., 2009. Direct observations of the ACC transport across the Kerguelen Plateau. Geophys. Res. Lett. 36, L18603, doi:10.1029/2009GL039617.

Patterson, T.A., Sharples, R.J., Raymond, B., Welsford, D.C., Andrews-Goff, V., Lea, M.A, Goldsworthy, S.D., Gales, N.J., Hindell, M. 2016. Foraging distribution overlap and

490 marine reserve usage amongst sub-Antarctic predators inferred from a multi-species
491 satellite tagging experiment. Ecol. Indic. 70, 531-544.
492 Pauly, T., Nicol, S., Higginbottom, I., Hosie, G., Kitchener, J. 2000. Distribution and
493 abundance of Antarctic krill (*Euphausia superba*) off East Antarctica (80–150 E) during
494 the Austral summer of 1995/1996. Deep-Sea Res. II 47, 2465-2488.
495 Pruvost, P., Duhamel, G., Palomares, M.L.D., 2005. An ecosystem model of the Kerguelen
496 Islands' EEZ. in: Palomares, M.L.D., Pruvost, P., Pitcher, T.J., Pauly, D. (Eds.),
497 Modeling Antarctic marine ecosystems. Fisheries Centre Research Reports 13 (7).
498 Fisheries Centre, University of British Columbia, Vancouver, Canada, pp 40−64.
499 Quinn, G.P., Keough, M.J., 2002. Experimental Design and Data Analysis for Biologists.
500 Cambridge University Press, Cambridge.
501 R Core Team, 2017. R: A language and environment for statistical computing. R Foundation
502 for Statistical Computing, Vienna, Austria.
503 Razouls, C., 1994. Manuel d'identification des principals espèces de copépods pélagiques
504 antarctiques et subantarctiques. Annales de L'Institut Océanographique 70, 1−204.
505 Roquet, F., Park, Y.-H., Guinet, C., Bailleul, F., Charrassin, J.-B., 2009. Observations of the
506 Fawn Trough Current over the Kerguelen Plateau from instrumented elephant seals. J.
507 Mar. Syst. 78, 377−393.
508 Schnack-Schiel, S.B., Hagen, W., 1995. Life-cycle strategies of *Calanoides acutus*, *Calanus*
509 *propinquus*, and *Metridia gerlachei* Copepoda: Calanoida in the eastern Weddell Sea,
510 Antarctica. ICES J. Mar. Sci. 52, 541−548.
511 Schnack-Schiel, S.B., Hagen, W., Mizdalski, E., 1991. Seasonal comparison of *Calanoides*
512 *acutus* and *Calanus propinquus* (Copepoda: Calanoida) in the southeastern Weddell
513 Sea, Antarctica. Mar. Ecol. Prog. Ser. 70, 17−27.
514 Smith, W.O. Jr, Ainley, D.G., Cattaneo-Vietti, R. 2007. Trophic interactions within the Ross

Sea continental shelf ecosystem. Phil. Trans. Royal Soc. London Series B, 362, 95-111.

Swadling, K.M., Kawaguchi, S., Hosie, G.W., 2010. Antarctic mesozooplankton community structure during BROKE-West (30°E−80°E), January–February 2006. Deep-Sea Res. II 57, 887−904.

Tachibana, A., Watanabe, Y., Moteki, M., Hosie, G.W., Ishimaru, T., 2017. Community structure of copepods in the oceanic and neritic waters off Adélie and George V Land, East Antarctica, during the austral summer of 2008. Polar Sci. 12, 34−45.

Takahashi, K.T., Hosie, G.W., Odate, T., 2017. Intra-annual seasonal variability of surface zooplankton distribution patterns along a 110ºE transect of the Southern Ocean in the austral summer of 2011/12. Polar Sci. 12, 46−58.

Tanimura, A., Kawaguchi, S., Oka, N., Nishikawa, J., Toczko, S., Takahashi, K.T., Terazaki, M., Odate, T., Fukuchi, M., Hosie, G., 2008. Abundance and grazing impacts of krill, salps and copepods along the 140°E meridian in the Southern Ocean during summer. Antarct. Sci. 20, 365−379.

Turner, J.A., Barrand, N.E., Bracegirdle, T.J., Convey, P., Hodgson, D.A., Jarvis, M., Jenkins, A., Marshall, G., Meredith, M.P., Roscoe, H., Shanklin, J., 2014. Antarctic climate change and the environment: an update. Polar Rec. 50, 237−259.

Wallis, J.R., Swadling, K.M., Everett, J.D., Suthers, I.M., Jones, H.J., Buchanan, P.J., Crawford, C.M., James, L.C., Johnson, R., Meiners, K.M., Virtue, P., Westwood, K., Kawaguchi, S., 2016. Zooplankton abundance and biomass size spectra in the East Antarctic sea-ice zone during the winter–spring transition. Deep-Sea Res. II 131, 170−181.

Ward, P., Atkinson, A., Venables, H.J. Tarling, G.A., Whitehouse, M.J., Fielding, S., Collins, M.A., Korb, R., Black, A., Stowasser, G., Schmidt, K., Thorpe, S.E., Enderlein, P., 2012. Food web structure and bioregions in the Scotia Sea: a seasonal synthesis. Deep-

Sea Res. II 59, 253−266.

Weatherall, P., Marks, K.M., Jakobsson, M., Schmitt, T., Tani, S., Arndt, J.E., Rovere, M., Chayes, D., Ferrini, V., Wigley, R., 2015. A new digital bathymetric model of the worlds oceans. Earth Space Sci. 2, 331−345.

Westwood, K., Pearce, I., 2018. Chlorophyll K-Axis Voyage V3 2015/16 Australian Antarctic Data Centre, doi:10.4225/15/5a94c701b98a8.

Wright, S.W., van den Enden, R.L., Pearce, I., Davidson, A.T., Scott, F.J., Westwood, K.J., 2010. Phytoplankton community structure and stocks in the Southern Ocean (30–80°E) determined by CHEMTAX analysis of HPLC pigment signatures. Deep-Sea Res. II 57, 758−778.

551 **Figure captions**

552 Fig. 1. Sampling stations along the Kerguelen Axis in the Southern Ocean during January and
553 February 2016.

554 Fig. 2. Hydrographic conditions along the Kerguelen Axis. (a) depth of surface mixed layer
555 (SML); (b) mean temperature in upper layer of SML averaged over the upper 20 dbar;
556 (c) average temperature over the top 200 m; (d) average salinity over the top 200 m; (e)
557 density averaged over the top 10 dbar: (f) chlorophyll *a* concentration averaged over the
558 top 150 dbar.

559 Fig. 3. Spatial distribution of total zooplankton abundance along the Kerguelen Axis during
560 January and February 2016.

561 Fig. 4. (a) Results of Q-mode clustering based on abundance of zooplankton community. Red
562 lines mean station groupings are not significant, as tested by SIMPROF. Labels show
563 sampling stations. (b) Abundance and species composition of groups based on the
564 cluster analysis at two similarity levels (from (a)). Error bars indicate standard
565 deviation around total abundance of each group. (c) Non-metric multi-dimensional
566 scaling (NMDS) plot with multiple regression analysis showing six groups based on the
567 cluster analysis. Vectors show significant environmental factors.

568 Fig. 5. Station groupings along the Kerguelen Axis, as determined from cluster analysis and
569 NMDS. Positions of frontal systems based on Bestley et al., 2018. ACC: Antarctic
570 Circumpolar Current; ASF: Antarctic Slope Front; FTC: Fawn Trough Current; SB:
571 Southern Boundary; SACCF: Southern Antarctic Circumpolar Current Front.

572 Fig. 6. Spatial distribution of dominant copepods along the Kerguelen Axis. Circle size and
573 colour denotes the abundance and mean copepodite stage of each species.

574

575 Table 1. Physical and biological variables included as predictors in the generalised linear
576 models (GLMs). Oceanographic variables (temperature, salinity and density) were all derived
577 from *in situ* CTD measurements undertaken at each RMT sampling site.

Variable	Explanation and source
Depth	Bathymetric depth (m) at sampling stations (Weatherall et al., 2015). Values are log10 transformed.
Chl.*a*	Integrated estimate of water column chlorophyll-*a* (mg m^{-2}; Westwood and Pearce, 2018) obtained using High Performance Liquid Chromatography following Wright et al. (2010), based on six CTD sampling depths within the upper 150 dbar.
Density	Mean potential density (kg m^{-3}) calculated relative to the surface (averaged over the upper 10 dbar). Low values (e.g. <26.8 kg m^{-3}) are indicative of recent ice influence/melt.
$Salinity_{200}$	Mean salinity over the depth between the surface and 200 m (the net sampling depth).
MLD	Mixed layer depth (m) estimates based on a change in density criterion of $\Delta\sigma\theta$=0.05 kg m^{-3} relative to 10 dbar, following de Boyer Montégut et al. (2004).
$Temp_{200}$	Mean temperature over the depth between the surface and 200 m (the net sampling depth).
Time since melt	The time since ice melted (days) calculated from daily passive microwave estimates of sea ice concentration (%) obtained from the National Snow and Ice Data Center SMMR-SSM/I polar product available for the Southern Hemisphere gridded at 25 km resolution (Cavalieri et al., 1996, updated yearly; Maslanik and Stroeve, 1999, updated daily).
SST	Mean near-surface water temperature (°C, averaged over the upper 20 dbar).
PAR	Ship-based measurement of PAR (photosynthetically active radiation, Watts m^{-2}) averaged from the port and starboard underway data during the RMT sampling periods.

578
579

580

581 Table 2. Mean abundance (1000 m^{-3}) for all species/taxon. **Bold** indicates IndVal of greater
582 than 25% for that group. * represents top 50% of species in each group according to SIMPER
583 analysis. Number in () represents N: number of sampling stations.

Species/taxon	Groups					
	A (4)	B (14)	C (2)	D (8)	E (7)	F (2)
Aetideopsis antarctica	0	1	0	0	1	0
Aetideopsis australis	0	0	**9**	0	0	0
Appendicularia	158	25	62	25	15	30
Calanoides acutus	**18223***	5836*	**34173***	607*	479	282*
Calanus nauplii	**1383**	109	444	164	7	0
Calanus propinquus	**6868***	3279*	**14628***	485*	468*	401*
Calanus simillimus	36	3	**1267**	0	0	**442***
Calanus spp. C1	**13345***	2895*	**16408**	468*	268	134*
Candacia sp.	**34**	0	9	0	0	1
Clausocalanus brevipes	**383**	205	**639**	37	38	13
Clausocalanus laticeps	62	26	9	5	0	**35**
Clio pyramidata forma *sulcata*	**223**	59	18	28	1	0
Clione limacina antarctica	0	**18**	0	1	4	0
Ctenocalanus spp.	**6847***	2165*	**6872***	285*	760*	458*
Cyllopus magellanicus	13	5	0	0	1	0
Euchirella rostromagna	**79**	24	9	5	5	1
Eukrohnia bathypelagica	0	5	**148**	1	0	0
Eukrohnia hamata	2690*	1809*	**6289***	355*	461*	186
Euphausia superba	0	32	**62**	1	21	0
Euphausia triacantha	0	0	**89**	0	0	0
Foraminifera	**28765***	9032*	**60372**	1072*	1255	124
Gaedius tenuispinus	13	7	0	2	4	0
Haloptilus longicirrus	**194**	41	0	2	6	2
Heterorhabdus austrinus	**353**	129	35	10	27	0
Hyperiella macronyx	88	9	**296**	6	0	42
Hyperiella sp.1(larva)	0	19	**148**	4	38	0
Isopoda	0	6	0	0	4	0
Limacina helicina	135	97	**157**	56	2	5
Limacina retroversa australis	0	0	18	1	0	**47**

Medusa	34	52	**157**	1	37	0
Metridia gerlachei	**2523**	1031	183	92	1088*	12
Metridia lucens	2831	627	**9925***	181	100	204*
Microcalanus pygmaeus	**237**	121	0	2	3	0
Oithona spp.	**10186***	1589*	**7458***	645*	276*	123*
Oncaea spp.	**3311***	1524*	**6621**	251*	308	81
Ostracoda	**809**	223	**1073**	54	139	3
Paraeuchaeta antarctica	**634**	166	**517**	17	168	6
Paraeuchaeta barbata	0	0	**9**	0	0	0
Pleuromamma robusta	57	7	**248**	9	5	0
Polychaeta	**1549**	406	**2070**	131	63	1
Primno macropa	72	**92**	44	5	43	1
Pseudochirella mawsoni	13	3	0	0	2	0
Racovitzanus antarcticus	554	147	**1931**	31	67	0
Radiolaria	1582	931*	**5293***	150	404*	209*
Rhincalanus gigas	**1714**	828	**2406***	104	378*	94
Rhincalanus gigas nauplii	2961*	776	**9352**	72	18	33
Sagitta gazellae	0	2	0	0	1	0
Sagitta marri	80	139	**349**	14	40	12
Sagitta maxima	0	13	**452**	0	5	3
Salp	**310**	82	**263**	11	53	0
Scaphocalanus farrani	**156**	35	18	4	3	0
Scaphocalanus vervoorti	**265**	28	0	0	29	0
Scina borealis	0	1	0	0	0	0
Scolecithricella minor	**642**	187	**946**	30	113	22
Scolecithricella ovata	**37**	4	0	0	0	0
Stephos longipes	**41**	12	0	1	0	1
Themisto gaudichaudii	**96**	10	18	4	20	26
Thysanoessa macrura	1642	945	**4927**	103	600*	60
Undinella brevipes	**13**	0	0	0	0	0
Urchin larva	0	26	**444**	0	2	0
Vibilia antarctica	25	2	0	0	1	0
Vibilia armata	0	0	0	2	0	**5**
Total abundance	112264	35844	196864	5531	7832	3101

584

Table 3. Result of GLM and "stepAIC" analysis for zooplankton abundance and mean copepodid stage along the Kerguelen Axis transect. If a variable is included in the model for a taxon it is shown as positive (up arrow) when higher abundances are associated with higher values of the variable and negative (down arrow) when higher abundances are associated with lower values of the variable. Int.: intercept, remaining variables as per Table 1. If a variable is included in the model for a taxon it is shown with an arrow -: p *: p <0.05; **: p <0.01; ***: p<0.001. MCS – mean copepodite stage.

	Intercept	Density	$Salinity_{200}$	SST	$Temp_{200}$	MLD	Depth	Chl.*a*	PAR	Time since melt	*p* value (ANOVA, null vs final)
Total zooplankton	*** ↑		*** ↓	*** ↓	*** ↑		*** ↓	*** ↑	** ↓		***
Amphipoda								* ↑			0.0605
Chaetognatha	*** ↑	*** ↓			** ↑		** ↓	*** ↑	** ↓		**
Copepoda	*** ↑		*** ↓	*** ↓	*** ↑		** ↓	*** ↑	** ↓		***
Euphausiacea	* ↑					* ↓	* ↓		- ↓		*
Foraminifera	*** ↑		*** ↓	*** ↓	*** ↑		*** ↓	*** ↑	** ↓		***
Copepods											
C. acutus	*** ↑	* ↓	** ↓		*** ↑		*** ↓	*** ↑	*** ↓	* ↓	***
C. propinquus	*** ↑		*** ↓	** ↓	*** ↑		*** ↓	*** ↑	*** ↓		***
M. gerlachei	** ↑		** ↓		*** ↓		- ↓	*** ↑	* ↓		***
M. lucens	** ↑		** ↓		*** ↑		** ↓	** ↑		* ↓	***

R. gigas	** ↑	* ↓			- ↑		* ↓	* ↑	** ↓		*
Mean copepodite stage											
MCS_*C. acutus*	** ↓	*** ↑			** ↓	** ↓		*** ↓		* ↑	***
MCS_*C. propinquus*	* ↑	*** ↑	*** ↓	*** ↓		- ↓	- ↓				***
MCS_*M. gerlachei*					- ↑						0.3302
MCS_*M. lucens*	*** ↑			** ↑			** ↓				***
MCS_*R. gigas*	** ↑					** ↓	- ↓		- ↑		**

590

591 Table 4. Summary of the important environmental dependencies evident in the models.
592

Model	Features
Total zooplankton abundance	Generally, higher abundances were associated with warmer temperatures, higher chlorophyll-*a* concentration and shallower depth, which was consistent with high abundances observed over the southern Kerguelen plateau (Fig. 3a). Lower abundances were associated with increased daylight.
Taxon abundances	Relationships mainly consistent with those reported for total zooplankton abundance. Additionally, chaetognaths were associated with surface low-Density. Higher abundances of euphausiids were associated with shallower mixed layer depths.
Large copepods	Relationships mainly consistent with those reported for total zooplankton abundance. However, *M. gerlachei* showed an opposite relation with temperature below the MLD. *C. acutus* and *M. lucens* were more abundant when there was a shorter time since sea-ice melt.
Copepod stages	The relationships varied with species.

593
594

595 Supplementary 1. Information about the sampling stations along the Kerguelen Axis in
596 the Southern Ocean during January and February 2016.

Station	Lat (S)	Long (E)	Date	Time (UTC)
KX04	63.473	93.551	23/01/16	09:56
KX05	62.998	93.590	23/01/16	17:24
KX07	61.718	93.327	24/01/16	07:44
KX08	61.134	93.595	24/01/16	18:43
KX09	61.976	92.536	25/01/16	07:16
KX12	62.470	87.158	27/01/16	07:44
KX13	62.482	85.887	27/01/16	20:07
KX14	62.530	83.905	28/01/16	07:21
KX15	62.529	81.949	28/01/16	23:57
KX16	63.292	82.042	29/01/16	20:20
KX17	63.930	83.065	30/01/16	11:08
KX18	64.345	83.633	31/01/16	09:48
KX19	64.410	84.769	01/02/16	05:30
KX20	65.172	85.330	01/02/16	22:32
KX22	65.042	91.494	02/02/16	21:50
KX23	64.318	89.843	03/02/16	14:12
KX24	63.607	88.232	04/02/16	01:14
KX25	63.133	87.259	04/02/16	15:43
KX26	62.502	86.128	04/02/16	22:16
KX27	61.936	85.035	05/02/16	11:23
KX28	61.222	83.863	06/02/16	00:31
KX29	60.363	82.496	06/02/16	13:27
KX30	59.344	81.073	07/02/16	09:14
KX31	58.648	80.160	07/02/16	21:33
KX32	58.223	81.912	08/02/16	10:19
KX33	57.930	83.353	08/02/16	21:47
KX34	57.608	84.608	09/02/16	10:05
KX35	57.839	85.290	09/02/16	19:01
KX37	59.101	84.411	10/02/16	16:21
KX38	60.027	86.750	11/02/16	10:34
KX39	60.052	85.833	11/02/16	23:54

KX40	60.319	83.580	12/02/16	13:41
KX42	60.910	79.882	13/01/16	15:03
KX43	61.317	77.592	14/02/16	08:26
KX44	61.846	74.115	15/02/16	01:28
KX45	62.704	73.314	15/02/16	10:46
KX47	64.866	71.177	16/02/16	07:51

597

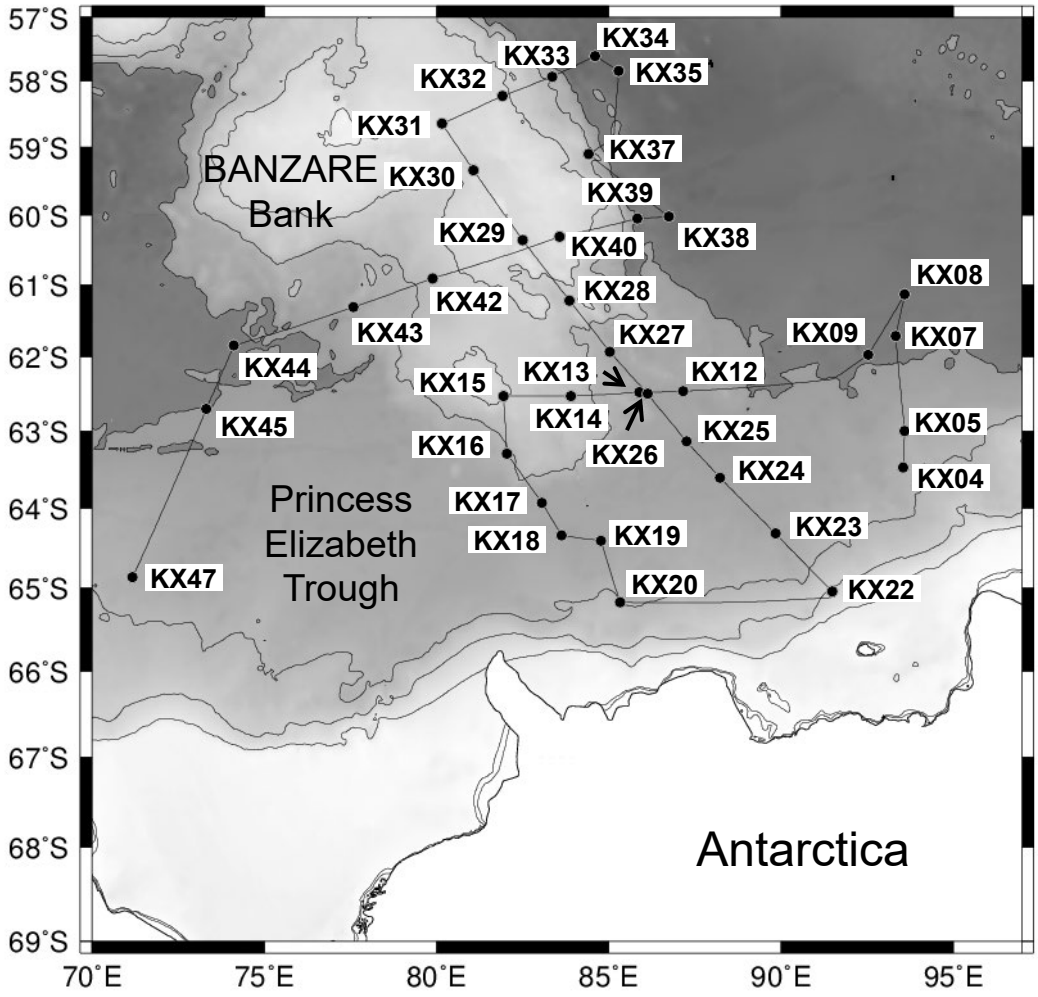

Fig. 1. (Matsuno et al.)

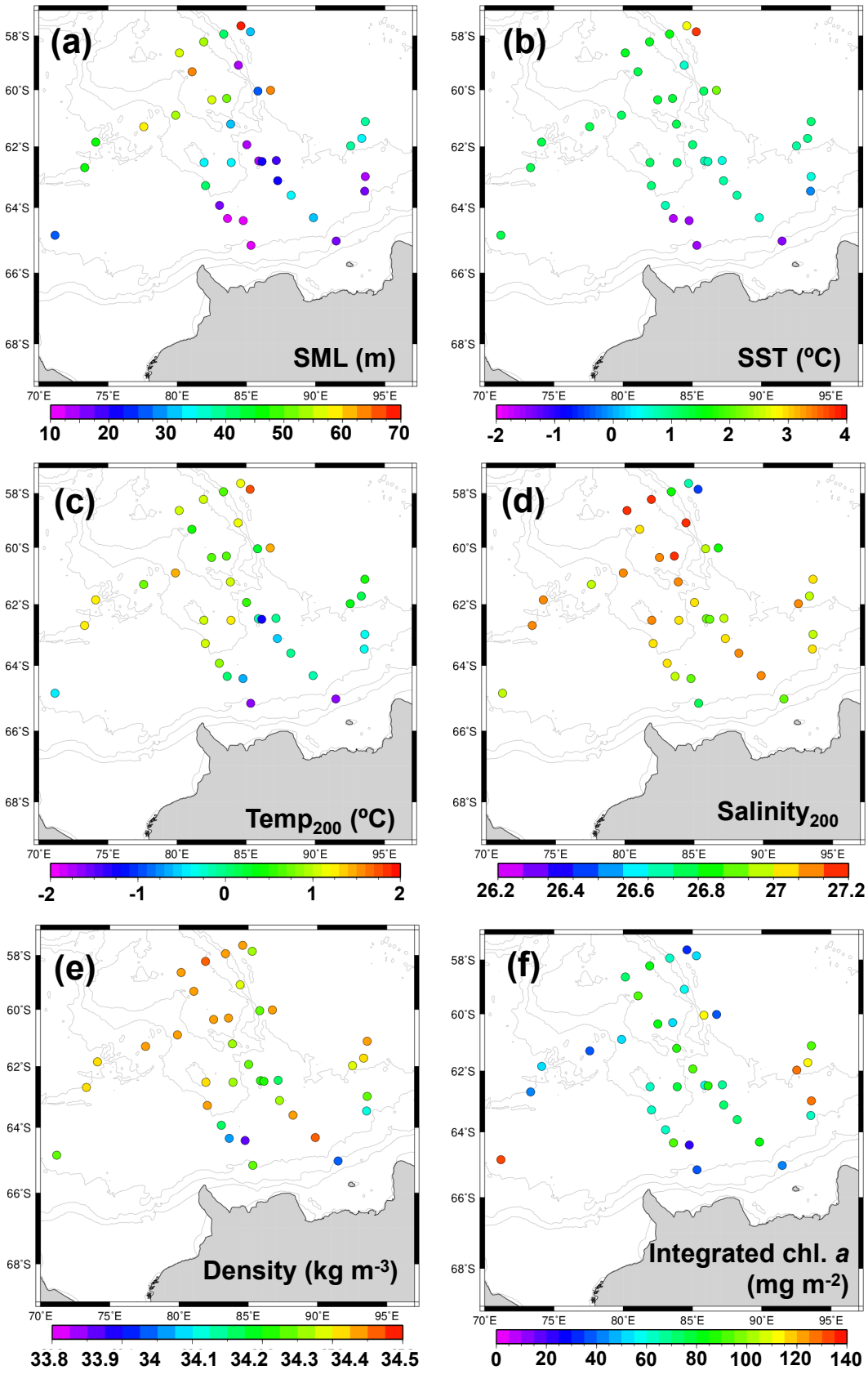

Fig. 2. (Matsuno et al.)

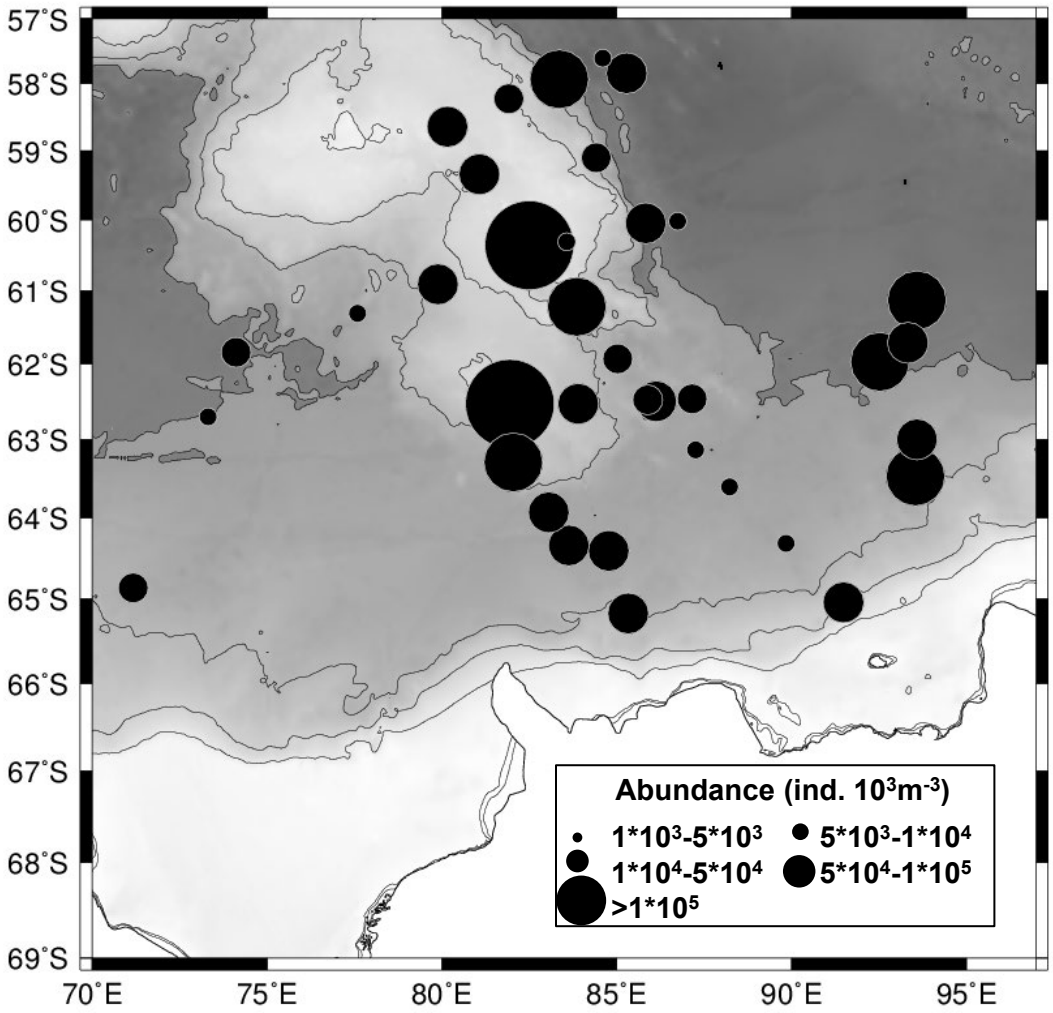

Fig. 3. (Matsuno et al.)

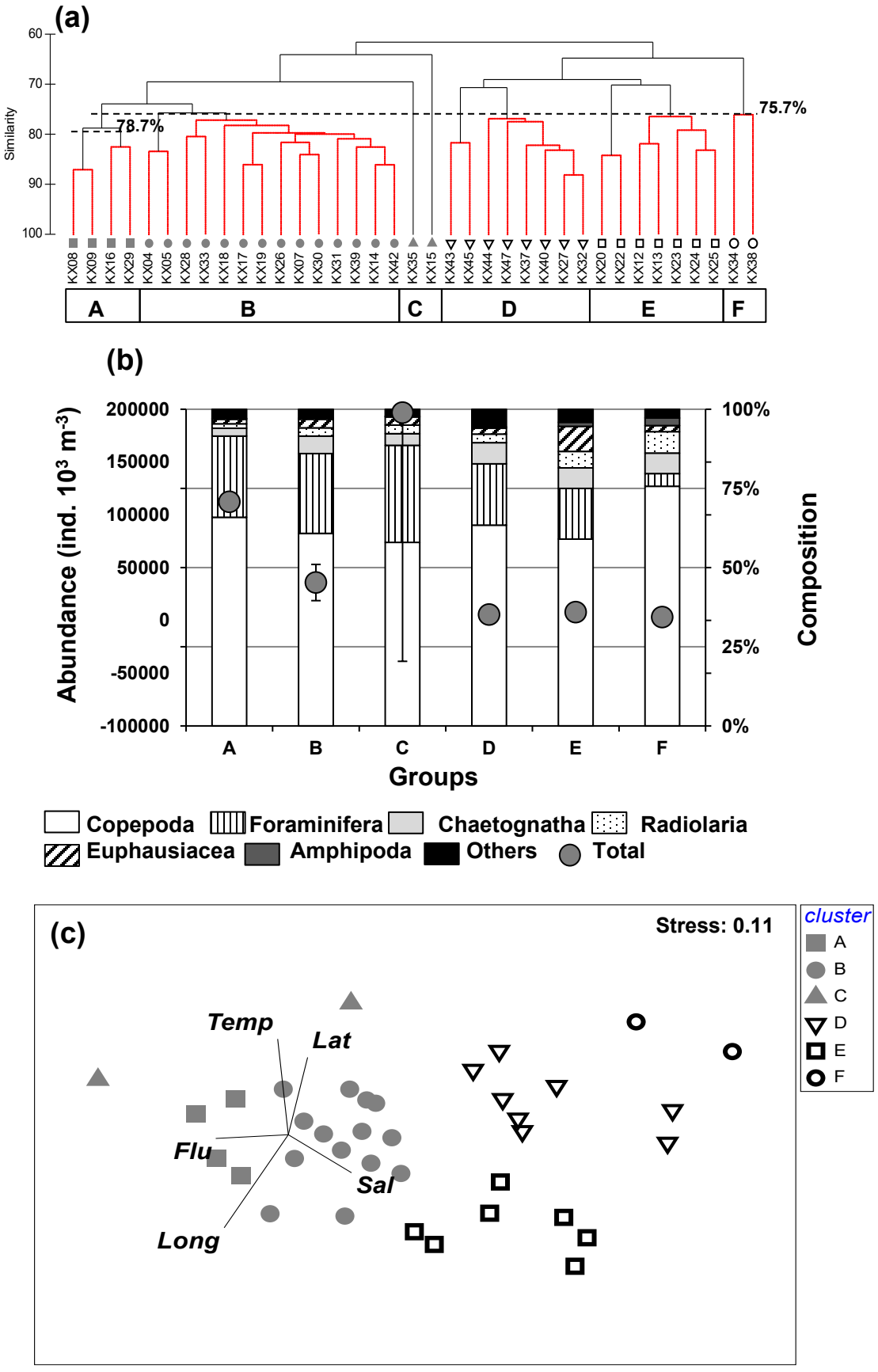

Fig. 4. (Matsuno et al.)

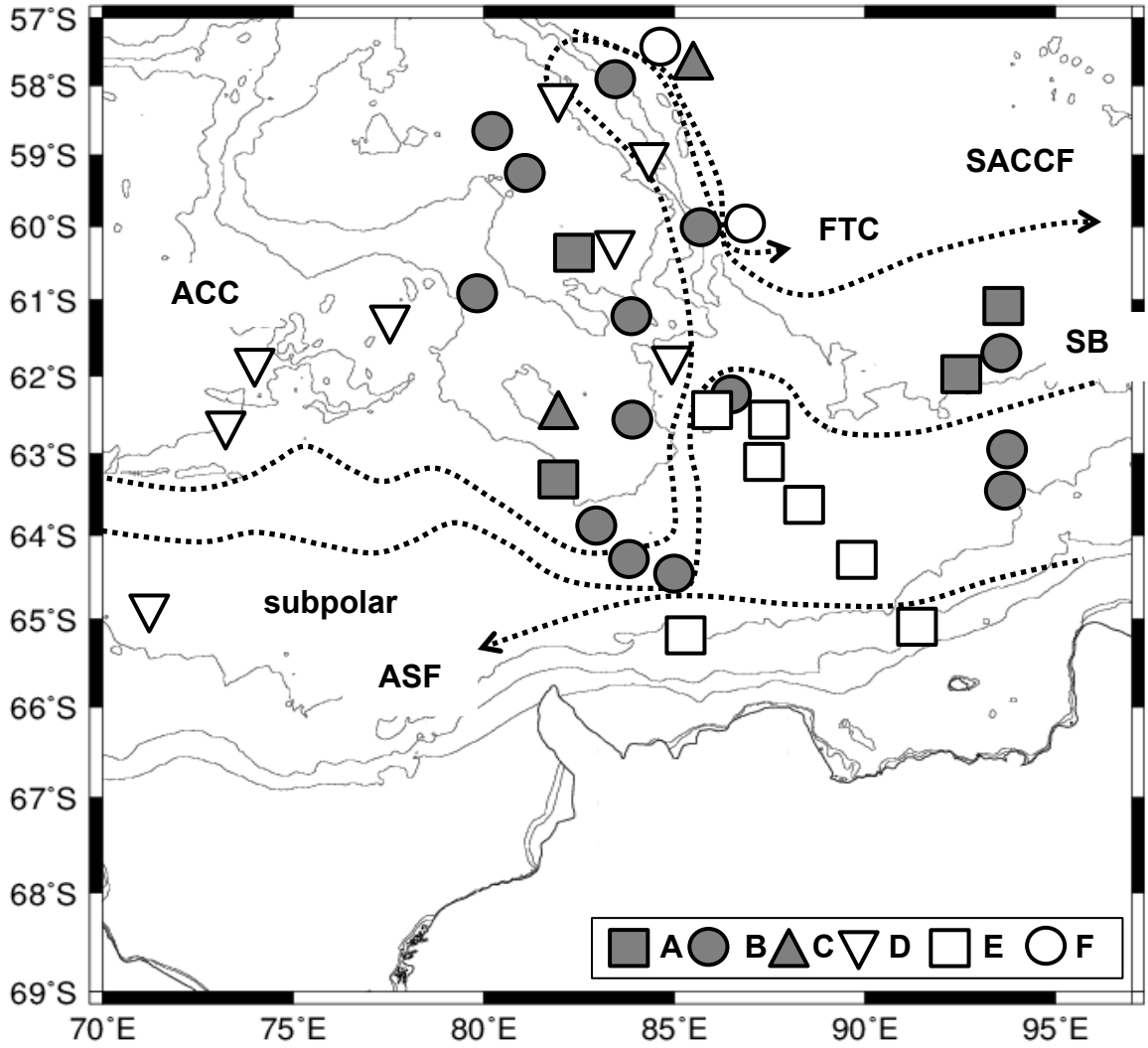

Fig. 5. (Matsuno et al.)

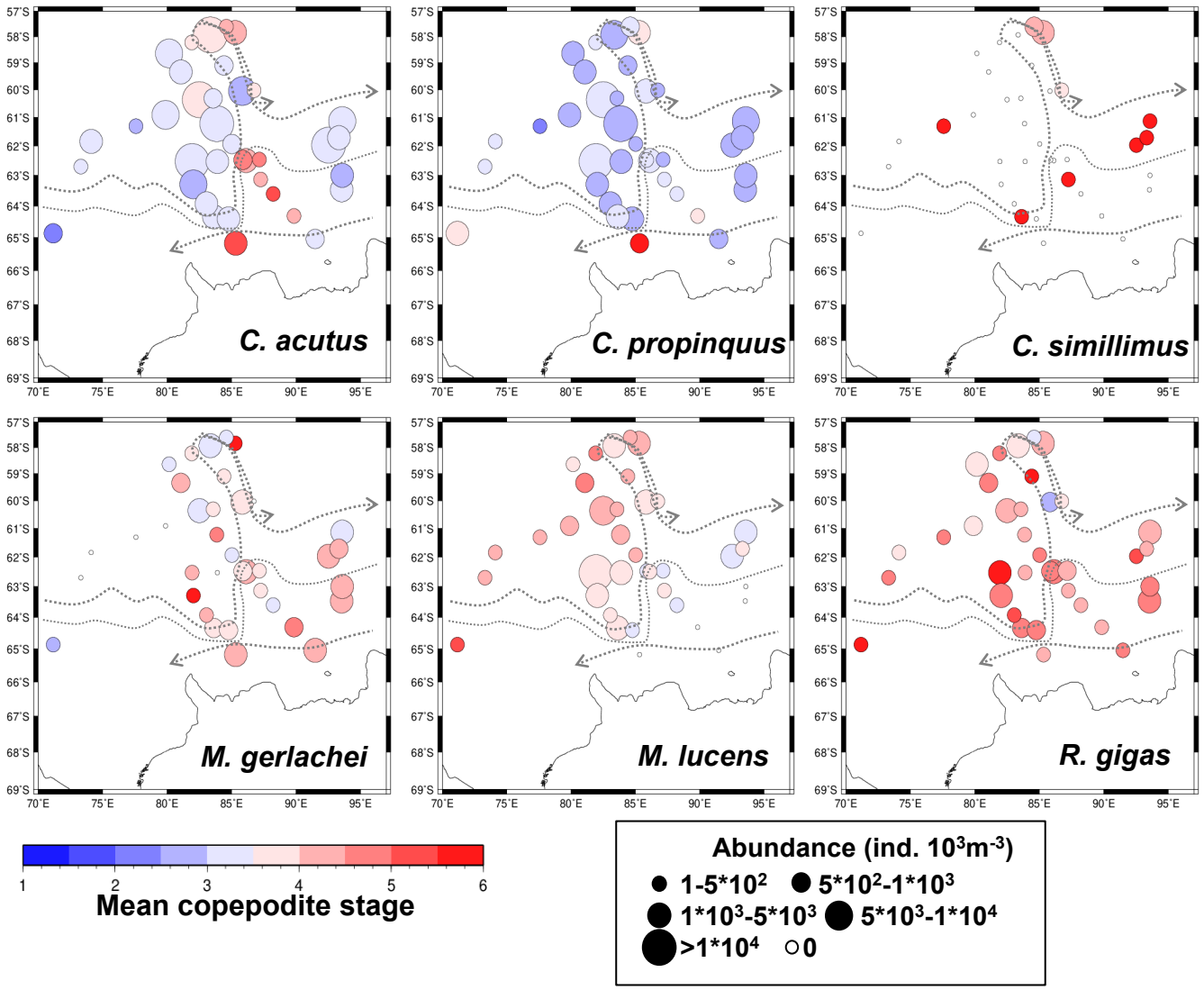

Fig. 6. (Matsuno et al.)